IMPROVED ILLUMINATION INVARIANT HOMOMORPHIC FILTERING USING THE DUAL TREE COMPLEX WAVELET TRANSFORM

P.R. Hill[1*], *H.Bhaskar*[2], *M.E. Al-Mualla*[2] *and D.R. Bull*[1]

[1]Electrical and Electronic Engineering, The University of Bristol, Bristol,BS8 1UB, UK
[2]Khalifa University of Science, Technology and Research (KUSTAR) P.O.Box 127788, Abu Dhabi, UAE

ABSTRACT

A novel adaptation of the two dimensional Homomorphic filter is introduced using the Dual Tree Complex Wavelet Transform for improved illumination invariant processing. The Homomorphic filter is conventionally implemented within the log-Fourier domain using an isotropic high-pass filter based on the assumption that the illumination signal occupies low spatial frequencies. In this case however, low frequency structural reflectance content will be incorrectly attenuated. Our method implements the Homomorphic filter using the DT-CWT and exploits the property of cross scale persistence (for structural content) to generate a filter that retains cross scale content and therefore reduces incorrect attenuation of structural reflectance content.

Index Terms— Wavelet, Homomorphic, Illumination

1. INTRODUCTION

Two dimensional Homomorphic filtering is a standard image enhancement technique that normalizes and stretches the contrast within an image while simultaneously attenuating image content attributable to surface illumination [1]. It is used in many imaging applications such as medical image enhancement [2–4], illumination invariant pre-processing for face recognition [5–8] and general image illumination normalisation [1]. Conventionally, Homomorphic filtering is implemented using an isotropic high pass filter (such as the Butterworth filter) within the Fourier domain [1]. However, recent work has used wavelet transforms [2, 3, 5–7].

Homomorphic filtering makes the following assumptions:

1. Illumination and reflectance are multiplicative.
2. High and low spatial frequency content is assumed to represent mostly reflectance and illumination respectively.

The Homomorphic filter initially takes the logarithm of image intensity making the illumination and reflectance components additive and therefore linearly separable in the frequency domain. A high pass filter is then used on the log intensity of the image. This filter suppresses low frequencies (and therefore illumination content) while amplifying high frequencies (and therefore reflectance content) within the log-intensity domain.

Frequency domain filtering can only affect global frequency content. We were therefore motivated to implement an identical spatial-domain filter in order to exploit localised spatial-frequency relationships and dependencies leading to a more optimal separation of illumination and reflectance content. We have developed such a filter using the Dual Tree Complex Wavelet Transform (DT-CWT) [9].

For conventional Homomorphic filtering, assumption 2 is a very generic presumption for all content. Our implemented filter uses the DT-CWT to exploit the property of cross scale persistence of structural reflectance thus preserving such content and more optimally separating the illumination and reflectance components.

This paper is organised as follows. Firstly, an overview of Homomorphic filtering, wavelets and wavelet based Homomorphic filtering is given in the remaining part of the introduction. This is followed by a description of the implemented DT-CWT based filter within section 2. Visual results of using this novel method are displayed together with quantitative comparisons against alternative methods within section 3. Finally a discussion and conclusion is presented in section 4.

1.1. Homomorphic filtering

A Lambertian illumination-reflectance model assumes that the intensity of an image $f(x, y)$ can be represented as the product of illumination $i(x, y)$ and reflectance $r(x, y)$, i.e.

$$f(x, y) = i(x, y)r(x, y), \tag{1}$$

where x and y are the spatial indices of the image pixels. As the Fourier transform of the product of two functions is not separable we define:

$$z(x, y) = \ln f(x, y) = \ln i(x, y) + \ln r(x, y), \tag{2}$$

$$Z(u, v) = F_i(u, v) + F_r(u, v), \tag{3}$$

where $F_i(u, v)$ and $F_r(u, v)$ are the Fourier transforms of $\ln i(x, y)$ and $\ln r(x, y)$ respectively. Additionally, u and v are the frequency indices in the x and y directions respectively. If we define our high pass filter as $H(u, v)$, then

$$\begin{aligned} S(u, v) = H(u, v)Z(u, v) = \\ H(u, v)F_i(u, v) + H(u, v)F_r(u, v), \end{aligned} \tag{4}$$

where $S(u, v)$ is the Fourier transform of the result. Transforming back to the spatial domain (where $\mathfrak{F}^{-1}$ is the inverse Fourier transform),

$$\begin{aligned} s(x, y) &= \mathfrak{F}^{-1}\{S(u, v)\} \\ &= \mathfrak{F}^{-1}\{H(u, v)F_i(u, v)\} + \mathfrak{F}^{-1}\{H(u, v)F_r(u, v)\} \end{aligned} \tag{5}$$

where the first term due to the illumination is expected to be attenu-

*Corresponding Author: paul.hill@bristol.ac.uk

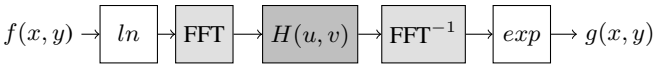

Fig. 1. Homomorphic filtering in the using the FFT

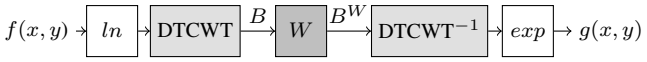

Fig. 2. Homomorphic filtering using the DTCWT

ated by the filter H. The output image can be expressed as

$$g(x,y) = e^{s(x,y)}. \tag{6}$$

$H(u,v)$ is commonly implemented using a circularly symmetric boosted Butterworth high pass filter [1] that can be defined as

$$H(u,v) = \left(1 - \frac{1}{\beta}\right) \frac{1}{1 + \left[\frac{D_0}{D(u,v)} + \right]^{2m}} + \frac{1}{\beta} \tag{7}$$

where $D(u,v)$ and D_0 are the radial frequency and the cutoff frequency respectively (both measured from the origin), β represents the relative high frequency boost and m determines the order of the filter. Although these parameters can be arbitrarily chosen, typical values of [$\beta = 3$, $D_0 = 0.3$ and $m = 2$] have been selected that gave good results in the experiments below. A cross section of the frequency response of $H(u,v)$ using these parameters is shown in Fig. 5. This shows the high-pass nature of the filter and how the low frequencies are attenuated leading to DC being reduced by a factor of 3 (from $\beta = 3$). A general block diagram of the algorithm is illustrated in Fig. 1.

1.2. Wavelet Based Homomorphic Filtering

Implementing the high pass filter H within the frequency domain only allows the frequency content to be modified globally. Spatial filters such as Difference of Gaussian (DoG) filters [8] and wavelets [2, 3, 5–7] have been used to locally implement the high pass filter H.

Yoon and Ro [4] have implemented H by simply weighting wavelet coefficients according to an equivalent Butterworth filter response at the central frequency of each subband. Similarly, Guta et al. [2] have just implemented hard and soft-thresholding constraints within all of the high pass wavelet subbands. Conversely, Gorgel et al. [3] have implemented an illumination normalisation system by implementing wavelet coefficient shrinkage on the high pass subbands and a separate Homomorphic filtering on the low pass subbands.

However, none of these methods have adequately exploited the spatial localisation of wavelet transforms and also have (in the majority of cases) used real valued wavelets that do not provide the improved characteristics of the DT-CWT exploited within our work.

1.3. The Dual Tree Complex Wavelet Transform (DT-CWT)

In order to adapt to local content, a spatial domain filter will need to be used. We have selected the DT-CWT over a conventional wavelet transform as it offers the following advantages.

- An efficient filter-bank implementation,
- Limited redundancy (4 to 1 for images),
- Shift-invariance,
- Improved directional selectivity over the conventional Discrete Wavelet Transform (DWT).

The DT-CWT is implemented using two decomposition trees using iterated Hilbert pairs of filters that form real and imaginary components for each of the six directionally orientated subbands [9].

2. IMPLEMENTATION

2.1. Homomorphic Filter using the DT-CWT

Fig. 2 shows our Homomorphic filter implemented using the DT-CWT. It mirrors the implementation shown in Fig. 1 but with the high-pass filter implemented using W, a weighted DT-CWT transform. W uses a forward and backward DT-CWT and weights the subband coefficients as follows.

The output of the DT-CWT in Fig. 2 is a set of indexed complex subbands $B = \{b_1, b_2, \ldots, b_n\}$. Where $n = 2 + 6J$ is the total number of subbands (J is number of decomposition levels[1]). The weight of each subband is calculated as

$$w_k = H(u_k, v_k), \tag{8}$$

where $k \in \{1, 2, \ldots, n\}$ and u_k and v_k define the maximum frequency response position of the basis function for subband k (calculated on a 512×512 grid). The output of the high pass filter W is therefore the set of subbands $B^W = \{b_1^W, b_2^W, \ldots, b_n^W\}$ where each b_k^W is defined as the product of the input subband b_k and the associated weight w_k calculated from (8):

$$b_k^W = b_k w_k \quad \text{for} \quad k = 1, 2, \ldots, n. \tag{9}$$

Fig. 5 shows the frequency response of the entire weighted DT-CWT 2D filter (sampled across the horizontal frequency axis) compared to $H(u,v)$. This shows that the filter implemented using the DT-CWT is a good match to $H(u,v)$. However, in order to make the filter have an even closer match to $H(u,v)$ we have generated modified weights w_{ck}. These modified weights are generated using the Nelder-Mead Simplex method [10] using the Chebyshev error as the objective function to be minimised across the two dimensional frequency domain (sampled across a grid of 512×512). Additionally, the following constraints are imposed on the minimisation process:

- The weights monotonically increase as wavelet scale increases (for each orientation),
- The weights for orientations +45° and -45° are assumed to be identical (for each wavelet scale),
- The weights for orientations +15°, -15°, +75° and -75° are assumed to be identical (for each wavelet scale),
- The DC weight ($H(0,0)$ given to the low pass subbands) is not changed and directly used to weight the low pass subbands.

The 2D Chebyshev error is defined as

$$\|E(u,v)\|_\infty = \max_{u \in [0,\pi], v \in [0,\pi]} |M(u,v)\,(W(u,v) - H(u,v))\,| \tag{10}$$

[1] J is set to 3 for all experiments within this paper

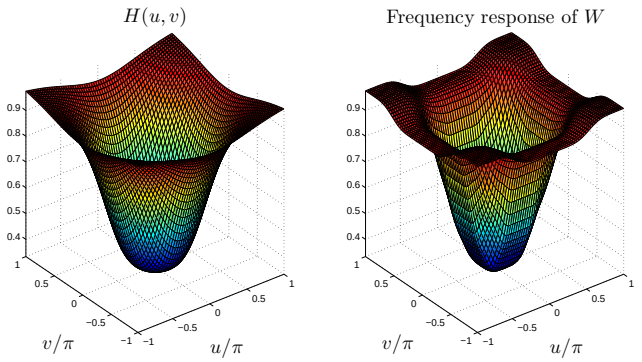

Fig. 3. 2D frequency response of $H(u,v)$ and W

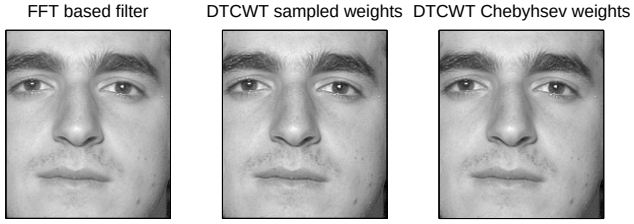

Fig. 4. Homomorphic filter implemented using FFT, DTCWT and DTCWT with Chebyshev weights (Original: **Im3** from Fig. 7).

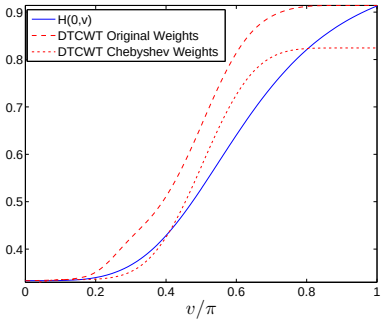

Fig. 5. Highpass filter using the FFT, DT-CWT with sampled weights and Chebyshev Weights (slice through $u = 0$ within Fig. 3)

where $W(u,v)$ and $H(u,v)$ are the sampled (on a grid of 512×512) frequency responses of W (including the forward and inverse DT-CWT) and H respectively. $M(u,v)$ is a weighting function defined as a 2D isotropic Gaussian with mean at the origin and $\sigma = 3$. This weighting function emphasises the importance of the central frequencies.

Fig. 3 shows the two dimensional surface representation of $H(u,v)$ for the parameters given above. Using the Chebyshev error method for obtaining the DT-CWT weights the two dimensional frequency response of the weighted DT-CWT is shown on the right of Fig. 3. Fig. 3 and Fig. 5 together show that the method is able to accurately model the shape of the Butterworth filter. Furthermore, Fig. 4 shows the output of three filters of the top left face shown in Fig. 7. This figure illustrates how the DT-CWT implementation of the Homomorphic filter is visually indistinguishable from the FFT version.

2.2. Cross-Scale Weighting of the DT-CWT based Filter

The sampled and Chebyshev-error based weights of the DT-CWT derived above will unnecessarily attenuate non-illumination content. It has been recognised that structural content within natural images results in high correlation across co-located coefficients within the wavelet domain [11, 12]. Within our work the weights w_{ck} are adjusted for each coefficient according to the co-located coefficient magnitudes of the child subband one scale higher in frequency ($c_{j-1,\theta}$) where j and θ are the scale and orientation of the considered coefficient. $c_{j-1,\theta}$ is defined as the magnitude of the co-located coefficient within the resized subband (using the Matlab `imresize` function). A more in depth description of cross-scale correspondences and models within the DT-CWT transform domain is given by Hill et al. [13].

2.2.1. Bayesian Estimation of Modified Weights

Cross-scale persistence of structural content has been exploited within wavelet based denoising algorithms [11]. This property can also be exploited to modify the weight w_{ck} of each coefficient in order to optimise Homomorphic filter attenuation; specifically to better retain structural coefficients where large magnitude child coefficients indicates content more likely attributable to structural / reflectance based content. Therefore we assume that the optimal weight o_{ck} of each coefficient is a linear sum of the given weight w_{ck} and an associated (uncorrelated) noise signal. Dropping the suffix ck for clarity and using Bayes' rule we obtain a *Maximum-a-Posteriori* (MAP) estimate for (o_{ck}):

$$\hat{o} = \arg\max_o P(o|w) = \arg\max_o P(w|o)P(o) \qquad (11)$$

For simplicity we assume both the likelihood $P(w|o)$ and prior $P(o)$ to be normally distributed.

$$\text{likelihood} \quad P(w|o) = \mathcal{N}(\mu_l, \sigma_l^2) \qquad (12)$$

$$\text{prior} \quad P(o) = \mathcal{N}(\mu_p, \sigma_p^2) \qquad (13)$$

The optimised weight ($\hat{o}$) is the MAP estimate of (11) given by the mean of the product distribution $P(w|o)P(o)$. After some simple manipulations we find

$$\hat{o} = \frac{\mu_l\sigma_p^2 + \mu_p\sigma_l^2}{\sigma_l^2 + \sigma_p^2}, \qquad (14)$$

where σ_l = 1, $\mu_l = w_{ck}$ and μ_p = 1. σ_p is defined as $1/c_{j-1,\theta}$. These parameter definitions ensure that the optimal weights $\hat{o}$ approach unity for large values of $c_{j-1,\theta}$. This enables coefficients that have co-located high frequency content to be less attenuated as they are assumed to be attributable to structural reflectance content. Conversely, as the value of $c_{j-1,\theta}$ decreases toward zero, the output weight $\hat{o}$ will approach the originally defined weight w_{ck} resulting in same level of filter attenuation as given in section 2.1.

3. RESULTS

3.1. Dataset

Fig. 6 and Fig. 7 show the images used for testing our approach. Image pairs 1-3 in Fig. 6 show three scenes captured from the Second Life rendering engine [14]. The first image (**Im1**) for each scene has no global illumination whereas the second image (**Im2**) has a

Table 1. PSNR and SSIM results for images shown in Fig. 6. All processing on **Im2**. All comparisons are from processed images to **Im1**.

		FFT Homomorphic	DT-CWT Homomorphic	DT-CWT Chebyshev	Bayesian DT-CWT
Image Pair 1	PSNR	11.7901	11.7657	11.9175	15.3485
	SSIM	0.7286	0.7260	0.7278	0.7573
Image Pair 2	PSNR	13.0228	12.9934	13.1841	17.5036
	SSIM	0.7571	0.7595	0.7577	0.8012
Image Pair 3	PSNR	10.0270	9.9982	10.1207	13.9505
	SSIM	0.6361	0.6329	0.6356	0.7232

global illumination generated from the sun and ambient occlusion. The lighting model within Second Life is generated using a Gaussian Bi-directional Reflectance Distribution Function (BRDF) [15]. The use of this model gives realistic illumination variations over a set of images while giving a precise (non illuminated) ground truth. Two pairs of faces are shown in Fig. 7. Each pair show the same face under two illumination conditions obtained from "The Extended Yale Face Database B" [16].

3.2. Comparison of Results

Fig. 6 shows the results of a range of Homomorphic filtering techniques of **Im2** (to be directly compared to **Im1**). The FFT based filter is able to attenuate the effect of illumination (each FFT Homomorphic filtered pair are consistently similar for all pairs). The Bayesian DT-CWT based method is able to retain more low pass information where there is high frequency content. Table 1 shows the PSNR and SSIM (the structural similarity metric [17]) values for the images shown in Fig. 6. This shows the difference between the processed versions of **Im2** and the original "non-illuminated" image **Im1**. This table shows that the DT-CWT Homomorphic and DT-CWT Chebyshev methods give virtually identical results (as expected) for all three image pairs. The Bayesian DT-CWT method gives significantly better results for both PSNR and SSIM.
The results in Fig. 7 further demonstrates that FFT Homomorphic filtering is able to attenuate the effect of illumination. However, (as above) the Bayesian DT-CWT method is able to retain more low pass information where there is also co-located high-frequency content.

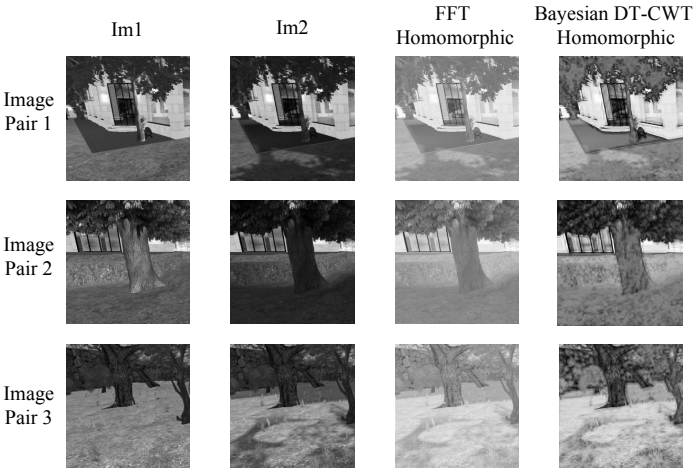

Fig. 6. Input and processed images. **Im1**: Input image 1 with no illumination, **Im2**: Input image 2 with GBRDF based illumination [15], **FFT**: Conventional Homomorphic filtering (of **Im2**), **Bayesian DT-CWT**: Homomorphic filtering (of **Im2**) implemented using Chebyshev-error together with the Bayesian cross scale method described in section 2.2

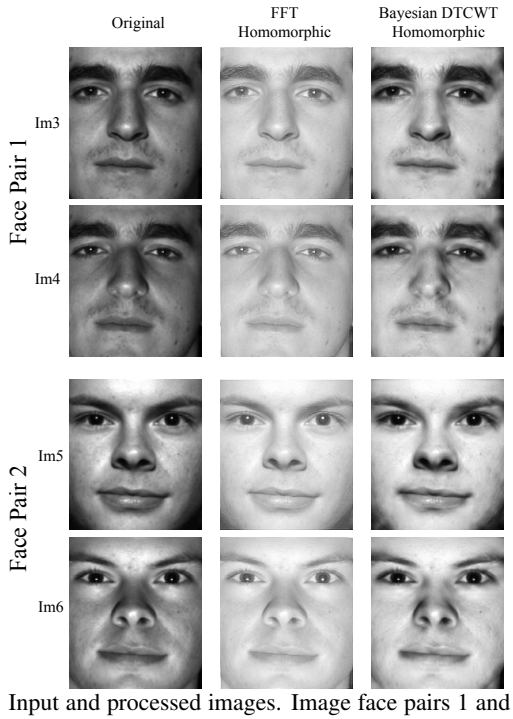

Fig. 7. Input and processed images. Image face pairs 1 and 2 show the same face under two illuminations. Both images are processed with FFT based and Bayesian DT-CWT Homomorphic filtering.

4. CONCLUSION

This paper has presented an improved Homomorphic filter for illumination invariant processing. It also proposes a 2D filter design structure to match a 2D frequency domain filter (in this case a Butterworth filter) with a weighted DT-CWT transform. The results of the new Bayesian DT-CWT based Homomorphic filter show considerable quantitative and qualitative improvements over the FFT based method while offering a flexible framework for implementing frequency domain spatial filtering.

Acknowledgement. We gratefully acknowledge funding of this work by Khalifa University of Science, Technology and Research (KUSTAR).

5. REFERENCES

[1] R.C. Gonzalez, and R.E. Woods, *Digital Image Processing (3rd Edition)*. Prentice-Hall, Inc., 2006.

[2] S. Gupta, R.C. Chauhan and S.C. Saxena, "Homomorphic wavelet thresholding technique for denoising medical ultrasound images," *Journal of Medical Engineering and Technology*, vol. 29, no. 5, pp. 208–214, 2005.

[3] P. Gorgel, A. Sertbas, and O.N. Ucan, "A wavelet-based mammographic image denoising and enhancement with homomorphic filtering," *Journal of Medical Systems*, vol. 34, no. 6, pp. 993–1002, 2010.

[4] J.H. Yoon and Y.M. Ro, "Enhancement of the contrast in mammographic images using the homomorphic filter method," *2012 International Conference on Electrical and Computer Engineering Advances in Biomedical Engineering*, vol. 85, no. 1, pp. 291–297, 2002.

[5] H. Han, S. Shan, X. Chen and W. Gao, "Illumination transfer using homomorphic wavelet filtering and its application to light-insensitive face recognition," *IEEE International Conference on Automatic Face Gesture Recognition*, pp. 1–6, September 2008.

[6] X. Yuan, Y. Meng, and X.-Y. Wei, "Illumination normalization based on homomorphic wavelet filtering for face recognition," *Journal of Information Science and Engineering*, vol. 29, no. 3, pp. 579–594, 2013.

[7] H. Hu, "Multiscale illumination normalization for face recognition using dual-tree complex wavelet transform in logarithm domain," *Computer Vision and Image Understanding*, vol. 115, no. 10, pp. 1384–1394, Oct 2011.

[8] C.-N. Fan and F.-Y. Zhang, "Homomorphic filtering based illumination normalization method for face recognition," *Pattern Recognition Letters*, vol. 32, no. 10, pp. 1468–1479, 2011.

[9] I.W. Selesnick, R.G. Baraniuk, and N.G. Kingsbury, "The Dual-Tree Complex Wavelet Transform," *IEEE Signal Processing Magazine*, vol. 22, no. 6, pp. 123–151, November 2005.

[10] J. C. Lagarias, J. A. Reeds, M. H. Wright, and P. E. Wright, "Convergence properties of the nelder-mead simplex method in low dimensions," *SIAM Journal of Optimization*, vol. 9, pp. 112–147, 1998.

[11] A. Achim, A. Loza, D. R. Bull and C. N. Canagarajah, "Statistical modelling for wavelet domain image fusion," *Image Fusion: Theory and Applications*, T. Sthathaki Ed., Academic Press 2008.

[12] L. Sendur and I. W. Selesnick, "Bivariate shrinkage functions for wavelet-based denoising exploiting interscale dependency," *IEEE Transactions on Signal Processing*, vol. 11, no. 50, pp. 2744–2756, Nov. 2002.

[13] P.R. Hill, A.M. Achim, D.R. Bull and M.E. Al-Mualla, "Dual-tree complex wavelet coefficient magnitude modelling using the bivariate Cauchy-Rayleigh distribution for image denoising," *Signal Processing*, vol. 105, pp. 464–472, 2014.

[14] Linden Lab, "Second Life." [Online]. Available: http://secondlife.com

[15] D. E. M. Kurt, "A Survey of BRDF Models for Computer Graphics," *SIGGRAPH*, vol. 43, no. 2, pp. 4:1–4:7, May 2009.

[16] K.-C. Lee, J. Ho, and D. Kriegman, "Acquiring linear subspaces for face recognition under variable lighting," *Pattern Analysis and Machine Intelligence, IEEE Transactions on*, vol. 27, no. 5, pp. 684–698, May 2005.

[17] Z. Wang, A. C. Bovik, H. R. Sheikh and E. P. Simoncelli, "Wavelets for Image Image quality assessment: From error visibility to structural similarity," *IEEE Transactions on Image Processing*, vol. 13, no. 4, pp. 600–612, April 2004.